

Anomalous nucleation of crystals within amorphous germanium nanowires during thermal annealing

O. Camara^{1,2}, A.H Mir¹, G. Greaves¹, S.E. Donnelly¹ and J.A. Hinks¹

¹School of Computing and Engineering, University of Huddersfield, Queensgate,
Huddersfield, HD1 3DH, United Kingdom

²Forschungszentrum Jülich GmbH, Institute of Energy and Climate Research -
Fundamental Electrochemistry (IEK-9), 52425 Jülich, Germany

Abstract

In this work, germanium nanowires rendered fully amorphous via xenon ion irradiation have been annealed within a transmission electron microscope to induce crystallization. During annealing crystallites appeared in some nanowires whilst others remained fully amorphous. Remarkably, even when nucleation occurred, large sections of the nanowires remained amorphous even though the few crystallites embedded in the amorphous phase were formed at a minimum of 200°C above the temperature for epitaxial growth and 100°C above the temperature for random nucleation and growth in bulk germanium. Furthermore, the presence of crystallites was observed to depend on the diameter of the nanowire. Indeed, the formation of crystallites occurred at a higher annealing temperature in thin nanowires compared with thicker ones. Additionally, nanowires with a diameter above 55 nm were made entirely crystalline when the annealing was performed at the temperature normally required for crystallization in germanium (i.e. 500°C). It is proposed that oxygen atoms hinder both the formation and the growth of crystallites. Furthermore, as crystallites must reach a minimum size to survive and grow within the amorphous nanowires, the instability of crystallites may also play a limited role for the thinnest nanowires.

Keywords: Crystallization; Nucleation and growth; Nanowires; Semiconductors; Transmission electron microscopy;

1.0 Introduction

Sparking enthusiasm since being first introduced in the literature as a new class of material [1], nanowires offer numerous novel properties compared with their bulk counterparts. In particular, semiconductor nanowires have already proven their worth as genuinely remarkable candidates for applications in electronic or optoelectronic devices [2]–[5].

In this respect, germanium nanowires are particularly interesting due to the high mobility of their charge carriers and to the possibility of engineering their band gap via combinations of strain and heavy doping [4], [6]–[8].

In most cases, the processing of semiconductors requires the modification of their electronic properties via doping [9], [10]. To do so, ion implanters are routinely used as a way of implanting chemical dopants within them [11], [12]. However, ion beams can induce damage to the target material and even lead to its amorphization [13]. Typically, to recover the crystalline character of the semiconductor a thermal annealing step is performed [14], [15]. In most cases the annealing step is considered crucial as the defects and the presence of localized electronic states in the valence and conduction bands of the amorphous phase can make the semiconductor unsuitable for the design of high performance electronic devices [16]–[18]. Nevertheless, complete or partial amorphization is almost inevitable when the processing of the semiconductor requires the implantation of a large concentration of dopants [19]. Additionally, the use of ion beams to purposely pre-amorphize semiconductors is preferred in order to better control the spatial distribution of the implanted dopants. Indeed, when ion implantation is performed on a crystalline material, the dopant profile is more difficult to predict due to effects such as ion channelling [20]. In fact, it has been shown that using a pre-amorphized semiconductor before

performing ion beam doping ultimately leads to better performance of the processed semiconductor after annealing [21].

In a single crystalline semiconductor that has undergone amorphization, a single crystal can be recovered during thermal annealing if a buried crystalline layer is preserved thus allowing solid phase epitaxial growth (SPEG) to occur [15]. In the absence of a crystalline “template”, crystalline seeds can nucleate within the amorphous layer at a higher temperature than that for SPEG [22], making the semiconductors polycrystalline as a result of the growth from the crystallites – a phenomenon known as random nucleation and growth (RNG) [22]. Whilst keeping a buried crystalline layer in bulk semiconductors specifically to enable SPEG after ion implantation is common, it is more challenging to do so during ion beam doping of nanowires as it requires that the ions induce only extremely shallow damage. Consequently, unless strategies such as shadowing sections of the nanowires (i.e. preventing sections of the nanowires from being bombarded by the ions [11]) or performing the irradiation at an elevated temperature to prevent amorphization are implemented [23], [24], RNG is to be expected under annealing. Typically, in bulk germanium SPEG is observed at 300°C and RNG around 400°C [25], [26].

In the current work, germanium nanowires have been amorphized via ion irradiation and subsequently subjected to thermal annealing in-situ in a transmission electron microscope (TEM). The temperature at which crystallization occurs in the nanowires is monitored in order to provide a comparison of the behaviour of the nanostructures with that of bulk material. Using in-situ TEM and electron energy loss spectroscopy (EELS), these experiments will aim to reveal an intriguing observation made in this work which may need to be taken into account when processing nanowires, that is, the fact that crystallization of germanium nanowires occurs at higher temperatures than that in the bulk and that this also depends on the nanowire diameter.

2.0 Methods

Single-crystal intrinsic germanium nanowires grown via vapour-liquid-solid (VLS) method on a silicon wafer were purchased from Nanowire Tech Ltd (product number GNWsI15). The commercially obtained nanowires were removed from the silicon wafer using an ultrasonic bath of ethanol at room temperature (RT) and subsequently dispersed onto either a TEM grid (molybdenum or nickel) with a carbon film or a TEM grid (molybdenum) with no film. The advantage of the film is that many more nanowires are captured on the grid and are thus available for TEM observation. The TEM grids with films have thus been used to obtain quantitative data regarding the proportion of nanowires crystallized at 500°C. Furthermore, having nanowires on the film and not deposited on the grid-bars ensures that the base of the nanowires are not shadowed from the ion beam by the grid-bars (thus making sure that they can be fully amorphized during irradiation). Indeed, even with careful sample preparation, when the nanowires are deposited directly on the grids, some might have their base located under the grid bars, meaning that the molybdenum grid can prevent the entirety of such nanowires becoming amorphous. On the other hand, TEM grids without a carbon film were used to record images, selected area diffraction patterns (SADPs) and EELS spectra without any “interference” from the film and materials that might have been sputtered onto it. The TEM grids without films were also used for control experiments – the aim of which was to confirm that the nucleation and growth was not inhibited as a result of a potentially-reduced thermal conduction between the carbon film and the nanowires (in contrast to that between the metal grid bars and nanowires). The diameters of the nanowires ranged between 10 and 100 nm whilst their length was between 100 nm and 2 μm .

The nanowires were irradiated at RT with 70 keV xenon ions up to a fluence of 6×10^{14} ion.cm^{-2} at which full amorphization was observed. The ion irradiations were performed at the Microscopes and Ion Accelerators for Materials Investigations (MIAMI-2) facility [27], which is equipped with a Hitachi H-9500 TEM operated at 300 kV maintaining a vacuum of 10^{-7} mbar and coupled to a 350 kV ion accelerator allowing in-situ ion irradiation.

The nanowires were considered fully amorphous when their SADPS showed only amorphous rings with no diffraction spots. Additional evidence of the microstructure of the nanowires was obtained using bright-field (BF) and dark-field (DF) TEM.

The nanowires were irradiated and annealed in-situ in the TEM using a Gatan Model 652 double-tilt heating holder. As the in situ annealing was performed directly after the in situ ion irradiation, the nanowires remained in the TEM during the whole experiments and contamination was thus minimised. During the annealing the nanowires used for quantitative analysis were incrementally heated and remained for at least 30 minutes at each of the following temperatures: 500°C, 510°C, 520°C, 530°C, 540°C, 560°C and 15 and 10 minutes at 580°C and 600°C, respectively.

3.0 Results and discussion

The SADPs were monitored during and after xenon irradiation in-situ in the TEM and showed that all the nanowires used in this work were fully amorphous. Following the irradiations, the nanowires were annealed to induce crystallization.

At 500°C, nucleation occurred in most of the nanowires for which the radius exceeded 25 nm. However, it must be noted that for nanowires for which the diameter did not exceed 55 nm, the nucleation and growth of crystallites was not induced in the entirety of the nanowires as they still had large sections which remained fully amorphous until annealing at a higher temperature was performed (i.e. up to 600°C in some cases). An example of such a nanowire after annealing at 500°C for 30 minutes is shown in the BF and DF-TEM images in Figure 1(a) and (b), respectively. In the BF-TEM image the amorphous region displays a relatively uniform contrast as compared with the crystallized region, which is the region close to the base of the nanowire and which appears bright in the DF-TEM image. The coexistence of a fully amorphous region and a region where crystallization has occurred is also confirmed by the SADPs in Figure 1 (a); as only amorphous rings are observed in the SADP taken from the amorphous region whilst the presence of a crystalline phase is evidenced by dark spots in the SADP of the region closest to the base of the nanowire. It must be noted that contrarily to the example shown in Figure 1, crystallization did not necessarily occur at the base of the nanowire. Indeed, during the in-situ annealing the crystalline sections seemed to be positioned randomly along each nanowires' length, (except when the nanowires had irregular diameters in which cases nucleation occurred first in the wider sections -see further examples of nanowires in the supplemental material, Figure S1).

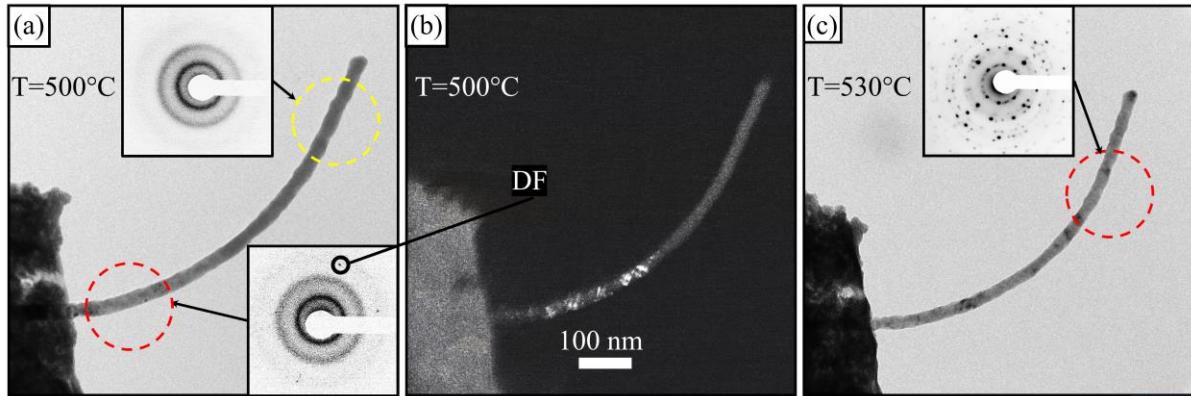


Figure 1. Micrographs showing (a) a BF and a (b) DF TEM image of a 28 nm diameter nanowire after annealing for 30 minutes at 500°C. The inset SADPs show evidence of the coexistence of both, crystalline and amorphous, phases at 500°C. (b) In the DF image, the bright contrast indicates the presence of crystal, thus showing further evidence that crystallization occurred at the base of the nanowire. (c) BF-TEM and SADP images of the nanowire at 530°C. The SADP of the nanowire show that the nanowire is now crystalline at 530°C. The selected area aperture positions are shown by the dashed circles yellow circles selecting fully amorphous regions and red circles those which are not. The scale bar in (b) also applies to images (a) and (c).

Qualitatively, it was observed that the highest temperatures facilitated the crystallization process as the proportions of nanowires exhibiting crystallites or becoming fully crystalline increased with the annealing temperature (until all nanowires became fully crystalline at 600°C). In some cases, nanowires were fully amorphous at 500°C and only started being partially crystalline at 560°C, thus corresponding to more than 3 hours of annealing at a temperature superior or equal to 500°C. In such instances it is reasonable to assume that the entirety of the TEM grid (and thus all nanowires) has reached the minimum temperature required for SPEG and RNG to occur in bulk materials. It must also be stated that the temperature within the nanowires rapidly reaches an equilibrium, thus: if nucleation occurs one might expect it to occur in the entire nanowire. Furthermore, it must be pointed out that the temperature required for the nucleation of a crystallite must not depend on the ion beam fluence. Indeed, whilst the structure of the amorphous phase may vary depending on the fluence, it has been shown that during

annealing at such temperatures, the amorphous phase undergoes a structural relaxation towards its lower energy form [28], [29]. Hence, at the relatively elevated temperatures used in the present work, the amorphous phase must be in its lower energy form and nucleation of crystallites should occur at the typical crystallization temperature (i.e. 500°C) and within the whole nanowires. Yet, as shown in the nanowire taken as example in Figure 1, this is not the case. Indeed, in this nanowire, nucleation first occurred at 500°C but it became fully crystalline at only 530°C – i.e. at a temperature more than 130°C above the typical temperature of RNG and 230°C above the typical temperature of SPEG in germanium as demonstrated in Figure 1(b) and (d) showing the DF image of the crystallized nanowire.

Furthermore, it was also observed that when nucleation occurred, it occurred within the first few minutes of each annealing step. As growth of a crystallite within a nanowire should take place similarly to what is observed during epitaxial growth of a crystallite in a bulk sample [30], [31], it is surprising that in several cases even after the nucleation of one or several crystallites within the first minutes of annealing, the growth of the crystallites did not make the entire nanowires crystalline during the 30 minute annealing step. For example, the amorphous section (i.e. the upper region) of the nanowire shown in Figure 1 became crystalline within the first 3 minutes of the 530°C annealing step. Using simple approximations (where the nanowire is considered cylindrical, the atomic density of germanium is 4.42×10^{22} atom per cm^3 and where the amorphous volume at 500°C can be estimated via the TEM micrographs) the number of germanium atoms rearranged into a crystalline phase at 530°C can be estimated to be $\approx 10^7$. This corresponds to a crystallization rate k_{530} of 5.5×10^4 atoms. s^{-1} . Using the Arrhenius equation and an activation energy of 2 eV for germanium recrystallization [25], it can be calculated that if the growth rate at 530°C is of 5.5×10^4 atoms. s^{-1} , at 500°C it should be equal to $\approx 1.8 \times 10^4$ atoms. s^{-1} . Consequently, such a growth rate at 500°C should be high enough to induce the germanium nanowire to become entirely crystalline (even without the nucleation of additional crystallites in the upper section of the nanowire).

Interestingly, whilst the crystallization process was clearly hindered, a trend related to the nanowire diameter was observed during annealing. In nanowires with smaller diameters, embedded crystalline grains were only observed at relatively-higher temperatures. Likewise, it was the thinner nanowires which necessitated the highest temperatures to become fully crystalline as only nanowires whose diameter was below 15 nm were not fully crystallized at a temperature of 580°C.

Whilst the mechanisms which cause the crystallization temperature to be relatively high will be addressed below, it is important to specify that a threshold diameter has been observed (i.e. 55 nm,) above which, the nanowires behaved like bulk germanium during thermal annealing as they became fully crystalline at 500°C. Furthermore, at 600°C all nanowires were crystalline, even the nanowires with the smallest diameter (i.e. 10 nm). Yet, although using an annealing temperature of 600°C can allow crystallization, the microstructure of the crystallized nanowire might be greatly influenced by the temperature ramp as crystallization does not occur uniformly on a given nanowire, at a given temperature.

Quantitatively, the correlation between the nanowire diameter and the presence of crystallites is most obvious when comparing the behaviour of nanowires whose diameter exceeded 25 nm with those below. As can be seen in Figure 2, most of the 15 nanowires with diameters below 25 nm were still fully amorphous at 500°C ($\approx 85\%$ of the nanowires with diameter below 25 nm). On the other hand, the Figure also shows that nucleation had occurred in most of the 27 nanowires whose diameter was above 25 nm at 500°C ($\approx 85\%$ of these thicker nanowires). This observation that nucleation is favoured in thicker nanowires is also in agreement with the observation that in nanowires whose diameter is uneven, nucleation occurs preferentially in the wider sections.

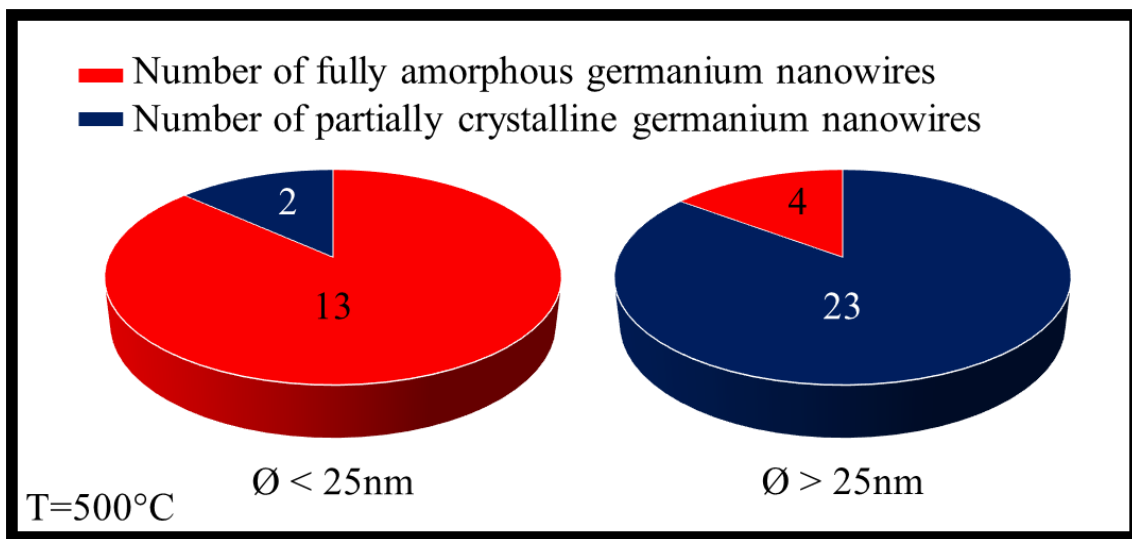


Figure 2. Comparison of populations of nanowires with diameters (\varnothing) above and below 25 nm which had partially crystallized at 500°C against those still fully amorphous.

The EELS spectra of nanowires (as for instance the spectra of the nanowire shown in Figure 1), revealed the presence of oxygen and thus the ratio of oxygen to germanium atoms at 500°C was determined. (The details of the calculation can be found in the supplemental material along with the EELS spectra shown in Figure S2). As germanium nanowires are surrounded by an oxide layer the presence of oxygen is not surprising. However, as expected under these conditions where the annealing is performed in the TEM columns under vacuum (i.e. at 10^{-7} mbar), the oxygen to germanium atomic ratio was only 0.2, meaning that major oxygen contamination of the specimen did not occur. Conversely, the atomic ratio would be 2 if the nanowires were converted into germanium oxide nanowires due to annealing under oxidizing atmosphere [32]. Therefore, it is clear that the relatively higher temperature of crystallization is indeed observed in germanium nanowires (and not in germanium oxide nanowires).

Nevertheless, the presence of oxygen can still play an important role in the inhibition of crystallization of the nanowires. Indeed, it has been previously shown that the presence of oxygen in silicon could retard epitaxial regrowth [33]. Consequently, in germanium, a similar effect of oxygen atoms has to be considered. In germanium, the supply of oxygen atoms within the nanowire can be directly provided by the oxide layer which plays the role of a source of oxygen atoms as the instability of the oxide layer has been reported to readily induce diffusion of oxygen from the oxide layer into the germanium at elevated temperatures (i.e. above 400°C) [34]. In nanowires, as the proportion of surface oxide is much greater than in bulk specimens (because of the high surface to volume ratio of the nanowires), the in-diffusion of oxygen will lead to a higher proportion of oxygen in the germanium nanowire than in a bulk specimen under similar conditions. Thus, oxygen diffusion will have a greater impact on the crystallization of the material. This may provide an explanation as to why nanowires remain largely amorphous even though the temperature is well above that which is typically required for both nucleation (i.e. the temperature for RNG is $\approx 400^\circ\text{C}$) and epitaxial growth from crystalline regions (i.e. the temperature for SPEG is $\approx 300^\circ\text{C}$) in bulk germanium. The influence of oxygen on the crystallization temperature due to the oxide layer acting as source of oxygen atoms agrees with the observation regarding the temperature of crystallization and the thickness of the nanowires. It should be noted that the oxide layers on the germanium nanowires were typically 3 nm thick regardless of the diameter of the nanowires. Consequently, one can deduce that the proportion of oxygen atoms is greater for thinner nanowires, thus providing a reasonable explanation on why crystallization temperature is higher for the thin nanowires as they are more likely to suffer from the effect of oxygen on crystallization. As stated above, crystallization is a crucial step performed after ion implantation during the processing of semiconductor based devices. For this processing step to be controlled, crystallization should occur at once and at a given temperature. Hence, the proportion of oxygen atoms in relatively thin germanium nanowires (i.e. those with a diameter below the threshold diameter) should be reduced to a minimum during annealing by stabilizing or removing the germanium native oxide layer.

It is worth noting that a similar correlation between nucleation and thickness has been reported previously during the annealing of amorphous germanium thin films [26], [35] but was attributed to the limited volume available for crystallization. The authors in [26] observed that for thin films of thickness below 30 nm, crystallization occurred at higher temperatures than in the bulk. They also observed that the thinner the film, the higher the crystallization temperatures (in the thinnest germanium film of 1 nm thick, crystals were formed only once a temperature of 550°C was reached). Furthermore, the same authors also reported that after annealing and formation of a few crystallites in the amorphous germanium thin film, subsequent growth did not occur.

It is known that even if a crystalline phase is formed, there will be a critical volume below which the crystallite is unstable and may thus dissolve and return to the amorphous state [18], [21]–[23]. Such an argument has been proposed in the literature to explain why crystallization may be less readily observed in thin films as compared with bulk [18], [21]–[23]. Indeed, the stability of a crystallite depends on whether its formation leads to an overall increase or decrease of energy. A crystallite will thus tend to dissolve if the phase transformation (i.e. crystallization) induces an increase in energy, whilst it will tend to grow if it induces an energy reduction. Thermodynamic considerations inherently associated with the phase transformation mean that for the crystallization to induce a reduction of energy, it must reach a minimum size at which, the energy reduction associated with the formation of a crystal is greater to the energy increase associated with the formation of an interface between the crystal and the amorphous phase [26]. In encapsulated thin films, the energy increase due to the interface depends on the material within which the thin film is encapsulated. Furthermore, the thinner the thin film the more the energy of the interface (and thus the critical size) depends on the encapsulating material. For these reasons, it has been observed that in several cases, reducing the film thickness can induce an increase of the critical size due to this influence of the encapsulating material on the interface energy. In such a scenario, using a higher crystallization temperature has been shown to induce a reduction of the critical volume (and thus allow the formation of smaller stable crystallites) [26], [36].

The critical volume has been proposed to explain why the thin germanium films [26] require a higher temperature for the formation of stable crystals [26], [36]. In the present work, a germanium nanowire

may be considered as being encapsulated within its oxide layer and an influence of this on the critical volume might be expected. However, in [26], for film thicknesses greater than or equal to 30 nm, the temperature of crystallization became similar to the bulk value (i.e. $\approx 400^\circ\text{C}$). This is in contrast to the present work where it has been observed that relatively large nanowires, such as nanowires with diameters up to 55 nm, had not fully crystallized after 30 minutes of annealing at 500°C , thus making the role of this mechanism questionable in such cases. However, for thinner nanowires, the role of the critical volume in the observed higher temperature of crystallization cannot be entirely dismissed.

It is to be expected that, in a nanowire, the influence of the oxide layer on the critical volume of a crystallite will be greater than it is for a thin film – the geometry of a nanowire as compared with that of a film means that, in a nanowire, the amorphous phase and the crystallite will not simply be encapsulated by two layers of oxide but will rather be enclosed within a cylindrical layer of oxide.

4.0 Conclusion

Following ion irradiation, the annealing of fully-amorphous germanium nanowires was performed within a TEM. During annealing, crystallites were formed at higher than expected temperatures (between 500°C and 600°C). The hindrance to crystallization has been mostly attributed to the indiffusion of oxygen originating in the oxide layer whilst the critical volume and temperature for crystallization may also play a limited role in this matter but only for the thinnest nanowires. Furthermore, a trend between the temperature at which the crystallites were formed and the diameter of the nanowires was observed as thinner nanowires required higher temperatures for nucleation and growth to occur. Conversely, a threshold diameter (i.e. 55 nm) has been observed above which, similarly to in the bulk, crystallization occurs in the whole nanowires at 500°C . Consequently, two strategies may be implemented: performing the thermal annealing above the threshold diameter or finding ways to limit the proportion of oxygen atoms in germanium nanowires (for instance, by reducing or removing the native oxide layer of the germanium nanowires).

Whilst future experiments will allow the precise correlation of the crystallization rate to the in-diffusion of oxygen originating from the surface layers, this work once more indicates how the high surface to bulk ratio of nanostructures can influence their properties and processing. Indeed, the results presented here reveal that whether nucleation is desired or unwanted, the temperature normally used for crystallization purposes in the bulk cannot necessarily be universally applied to nanowires. Consequently, for crystallisation purposes, this work shows that annealing should be performed

Acknowledgement

The construction of the MIAMI-2 was funded by the Engineering and Physical Sciences Research Council, United Kingdom under grant number EP/M028283/1.

- [1] R. S. Wagner and W. C. Ellis, "VAPOR-LIQUID-SOLID MECHANISM OF SINGLE CRYSTAL GROWTH," *Appl. Phys. Lett.*, vol. 4, no. 5, pp. 89–90, Mar. 1964, doi: 10.1063/1.1753975.
 - [2] Y. Cui, Z. Zhong, D. Wang, W. U. Wang, and C. M. Lieber, "High performance silicon nanowire field effect transistors," *Nano Lett.*, vol. 3, no. 2, pp. 149–152, 2003, doi: 10.1021/nl025875l.
 - [3] Y. Li *et al.*, "Dopant-free GaN/AlN/AlGaIn radial nanowire heterostructures as high electron mobility transistors," *Nano Lett.*, vol. 6, no. 7, pp. 1468–1473, 2006, doi: 10.1021/nl060849z.
 - [4] J. Greil, A. Lugstein, C. Zeiner, G. Strasser, and E. Bertagnolli, "Tuning the electro-optical properties of germanium nanowires by tensile strain," *Nano Lett.*, vol. 12, no. 12, pp. 6230–6234, 2012, doi: 10.1021/nl303288g.
 - [5] F. Priolo, T. Gregorkiewicz, M. Galli, and T. F. Krauss, "Silicon nanostructures for photonics and photovoltaics," *Nat. Nanotechnol.*, vol. 9, no. 1, pp. 19–32, 2014, doi: 10.1038/nnano.2013.271.
 - [6] D. Wang *et al.*, "Germanium nanowire field-effect transistors with SiO₂ and high- κ HfO₂ gate dielectrics," *Appl. Phys. Lett.*, vol. 83, no. 12, pp. 2432–2434, 2003, doi: 10.1063/1.1611644.
 - [7] G. Scappucci, G. Capellini, W. M. Klesse, and M. Y. Simmons, "New avenues to an old material: Controlled nanoscale doping of germanium," *Nanoscale*, vol. 5, no. 7, pp. 2600–2615, 2013, doi: 10.1039/c3nr34258a.
 - [8] L. Seravalli *et al.*, "Extra-long and taper-free germanium nanowires: Use of an alternative Ge precursor for longer nanostructures," *Nanotechnology*, vol. 30, no. 41, 2019, doi: 10.1088/1361-6528/ab31cf.
 - [9] J. R. Weber, A. Janotti, and C. G. Van de Walle, "Defects in Germanium," in *Photonics and Electronics with Germanium*, K. Wada and L. C. Kimerling, Eds. Weinheim, Germany: Wiley-VCH Verlag GmbH & Co. KGaA, 2015, pp. 1–23.
-

- [10] R. A. Kelly, J. D. Holmes, and N. Petkov, "Visualising discrete structural transformations in germanium nanowires during ion beam irradiation and subsequent annealing," *Nanoscale*, vol. 6, no. 21, pp. 12890–12897, 2014, doi: 10.1039/c4nr04513k.
- [11] R. A. Kelly *et al.*, "Epitaxial Post-Implant Recrystallization in Germanium Nanowires," *Cryst. Growth Des.*, vol. 15, no. 9, pp. 4581–4590, 2015, doi: 10.1021/acs.cgd.5b00836.
- [12] Y. Berencén *et al.*, "Formation of n- and p-type regions in individual Si/SiO₂ core/shell nanowires by ion beam doping," *Nanotechnology*, vol. 29, no. 47, 2018, doi: 10.1088/1361-6528/aadfb6.
- [13] L. Pelaz, L. A. Marqués, and J. Barbolla, "Ion-beam-induced amorphization and recrystallization in silicon," *J. Appl. Phys.*, vol. 96, no. 11, pp. 5947–5976, 2004, doi: 10.1063/1.1808484.
- [14] P. D. Edmondson, D. J. Riley, R. C. Birtcher, and S. E. Donnelly, "Amorphization of crystalline Si due to heavy and light ion irradiation," *J. Appl. Phys.*, vol. 106, no. 4, pp. 1–8, 2009, doi: 10.1063/1.3195081.
- [15] A. Claverie, S. Koffel, N. Cherkashin, G. Benassayag, and P. Scheiblin, "Amorphization, recrystallization and end of range defects in germanium," *Thin Solid Films*, vol. 518, no. 9, pp. 2307–2313, 2010, doi: 10.1016/j.tsf.2009.09.162.
- [16] T. T. Tran, J. Wong-Leung, L. A. Smillie, A. Hallen, M. G. Grimaldi, and J. S. Williams, "Non-localized states and high hole mobility in amorphous germanium. (arXiv:1908.08246v1 [cond-mat.mtrl-sci])," *arXiv Mater. Sci.*, pp. 1–10, [Online]. Available: <http://arxiv.org/abs/1908.08246>.
- [17] P. A. Walley and A. K. Jonscher, "In amorphous germanium," vol. 1, pp. 367–377, 1967.
- [18] R. W. Miles, K. M. Hynes, and I. Forbes, "Photovoltaic solar cells: An overview of state-of-the-art cell development and environmental issues," *Prog. Cryst. Growth Charact. Mater.*, vol. 51, no. 1–3, pp. 1–42, 2005, doi: 10.1016/j.pcrysgrow.2005.10.002.
- [19] O. Camara, M. A. Tunes, G. Greaves, A. H. Mir, S. Donnelly, and J. A. Hinks, "Understanding amorphization mechanisms using ion irradiation in situ a TEM and 3D damage reconstruction," *Ultramicroscopy*, vol. 207, no. August, p. 112838, 2019, doi: 10.1016/j.ultramic.2019.112838.
- [20] N. Ohno, T. Hara, Y. Matsunaga, M. I. Current, and M. Inoue, "Diffusion of ion-implanted boron impurities into pre-amorphized silicon," *Mater. Sci. Semicond. Process.*, vol. 3, no. 3, pp. 221–225, 2000, doi: 10.1016/S1369-8001(00)00036-6.
- [21] V. Vervisch *et al.*, "Laser activation of Ultra Shallow Junctions (USJ) doped by Plasma Immersion Ion Implantation (PIII)," *Appl. Surf. Sci.*, vol. 255, no. 10, pp. 5647–5650, 2009, doi: 10.1016/j.apsusc.2008.11.010.
- [22] R. Duffy *et al.*, "Solid phase epitaxy versus random nucleation and growth in sub- 20 nm wide fin field-effect transistors," *Appl. Phys. Lett.*, vol. 90, no. 24, pp. 88–91, Jun. 2007, doi: 10.1063/1.2749186.
- [23] N. Fukata, R. Takiguchi, S. Ishida, S. Yokono, S. Hishita, and K. Murakami, "Recrystallization and reactivation of dopant atoms in ion-implanted silicon nanowires," *ACS Nano*, vol. 6, no. 4, pp. 3278–3283, 2012, doi: 10.1021/nn300189z.
- [24] O. Camara *et al.*, "Effects of temperature on the ion-induced bending of germanium and silicon nanowires," *Mater. Res. Express*, vol. 4, no. 7, 2017, doi: 10.1088/2053-1591/aa7e05.
- [25] L. Csepregi, R. P. P. Küllen, J. W. W. Mayer, and T. W. W. Sigmon, "Regrowth kinetics of amorphous Ge layers created by ⁷⁴Ge and ²⁸Si implantation of Ge crystals," *Solid State*
-

- Commun.*, vol. 21, no. 11, pp. 1019–1021, Mar. 1977, doi: 10.1016/0038-1098(77)90009-6.
- [26] G. Radnóczy and B. Pécz, “Crystallization of encapsulated very thin amorphous Ge layers,” *Thin Solid Films*, vol. 232, no. 1, pp. 68–72, 1993, doi: 10.1016/0040-6090(93)90764-G.
- [27] G. Greaves, A. H. H. Mir, R. W. W. Harrison, M. A. A. Tunes, S. E. E. Donnelly, and J. A. A. Hinks, “New Microscope and Ion Accelerators for Materials Investigations (MIAMI-2) system at the University of Huddersfield,” *Nucl. Instruments Methods Phys. Res. Sect. A Accel. Spectrometers, Detect. Assoc. Equip.*, vol. 931, no. December 2018, pp. 37–43, 2019, doi: 10.1016/j.nima.2019.03.074.
- [28] C. E. Bouldin, R. A. Forman, M. I. Bell, and E. P. Donovan, “Structural relaxation in ion-damaged amorphous germanium,” *Phys. Rev. B*, vol. 44, no. 11, pp. 5492–5496, Sep. 1991, doi: 10.1103/PhysRevB.44.5492.
- [29] N. N. Dong, J. G. Xu, J. J. Cui, and X. Wang, “Structural relaxation probed by resistance drift in amorphous germanium,” *Mater. Res. Express*, vol. 7, no. 3, 2020, doi: 10.1088/2053-1591/ab80a9.
- [30] O. Camara *et al.*, “Shape Modification of Germanium Nanowires during Ion Irradiation and Subsequent Solid-Phase Epitaxial Growth,” *Adv. Mater. Interfaces*, vol. 5, no. 13, 2018, doi: 10.1002/admi.201800276.
- [31] R. A. Kelly, J. D. Holmes, and N. Petkov, “Visualising discrete structural transformations in germanium nanowires during ion beam irradiation and subsequent annealing. Supporting material,” *Nanoscale*, vol. 6, no. 21, pp. 12890–7, 2014, doi: 10.1039/c4nr04513k.
- [32] N. TABET, J. AL-SADAH, and M. SALIM, “GROWTH OF OXIDE LAYER ON GERMANIUM (011) SUBSTRATE UNDER DRY AND WET ATMOSPHERES,” *Surf. Rev. Lett.*, vol. 06, no. 06, pp. 1053–1060, Dec. 1999, doi: 10.1142/S0218625X99001141.
- [33] E. F. Kennedy, L. Csepregi, J. W. Mayer, and T. W. Sigmon, “Influence of ^{16}O , ^{12}C , ^{14}N , and noble gases on the crystallization of amorphous Si layers,” *J. Appl. Phys.*, vol. 48, no. 10, pp. 4241–4246, 1977, doi: 10.1063/1.323409.
- [34] G. Copetti, G. V. Soares, and C. Radtke, “Stabilization of the GeO_2/Ge Interface by Nitrogen Incorporation in a One-Step NO Thermal Oxynitridation,” *ACS Appl. Mater. Interfaces*, vol. 8, no. 40, pp. 27339–27345, 2016, doi: 10.1021/acsami.6b09244.
- [35] G. Garcia *et al.*, “Crystallisation of Amorphous Germanium Thin Films,” *J. Nanosci. Nanotechnol.*, vol. 9, no. 5, pp. 3013–3019, May 2009, doi: 10.1166/jnn.2009.225.
- [36] J. A. Venables and G. D. T. Spiller, “Nucleation and Growth of Thin Films,” *Surf. Mobilities Solid Mater.*, vol. 47, no. 4, pp. 341–404, 1983, doi: 10.1007/978-1-4684-4343-1_16.
- [37] R. F. Egerton, *Electron energy loss spectroscopy in the microscope*, 3rd Ed. Springer, 2011.
-